

This is the peer reviewed version of the following article: [Antonio Cascella, Sergio Bonomo, Bassem Jalali, Marie-Alexandrine Sicre, Nicola Pelosi, Sabine Schmidt, Fabrizio Lirer (2019). Climate variability of the last 2700 years in the Southern Adriatic Sea: Coccolithophore evidences. The Holocene, which has been published in final form at [doi.org/10.1177/0959683619865]. This article may be used for non-commercial purposes in accordance with SAGE Terms and Conditions for Self-Archiving.

1
2
3
4
5
6
7
8
9
10
11
12
13
14
15
16

Climate variability of the last ~2700 years in the Southern Adriatic Sea:

Coccolithophore evidences

Antonio Cascella^{1*}, Sergio Bonomo¹⁻²⁻³, Bassem Jalali⁴, Marie-Alexandrine Sicre⁴, Nicola Pelosi²,
Sabine Schmidt⁵, Fabrizio Lirer²

1) Istituto Nazionale di Geofisica e Vulcanologia (INGV), Via della Faggiola 32, 52126, Pisa;*
corresponding author: antonio.cascella@ingv.it

2) Istituto di Scienze Marine (ISMAR), Consiglio Nazionale delle Ricerche (CNR), Calata Porta di
Massa, Interno Porto di Napoli, 80133- Naples, Italy.

3) Istituto di Biomedicina ed Immunologia Molecolare "Alberto Monroy" (IBIM), Consiglio
Nazionale delle Ricerche, Via Ugo La Malfa 153, 90146, Palermo, Italy;

4) Sorbonne Universités (UPMC, Univ. Paris 06) CNRS-IRD-MNHN, LOCEAN Laboratory, 4 place
Jussieu, F-75005 Paris, France;

5) UMR5805 EPOC, Université de Bordeaux, Avenue Geoffroy Saint-Hilaire, 33615 Pessac, France;

17

18 **Abstract**

19 New information on paleoenvironmental conditions over the past ~2700 years in the Central
20 Mediterranean Sea have been acquired through the high-resolution study of calcareous
21 nanofossils preserved in the sediment core SW104ND14Q recovered in the Southern
22 Adriatic Sea (SAS) at 1013 m water depth. The surface water properties at this open SAS site
23 are sensitive to atmospheric forcing (acting both at local and regional scale) and the North
24 Ionian Sea driven inflowing waters. Our data show a relationship between reworked coccolith
25 abundances, flood frequency across the Southern Alps and the North Atlantic Oscillation
26 (NAO) confirming their value as indicator of runoff/precipitation. Changes in the abundance
27 of the opportunistic (r-strategist) species *Emiliania huxleyi* and deep dweller taxa
28 *Florisphaera profunda* were used to reconstruct the upper water column stratification and
29 associated changes in coccolithophorid productivity. The negative correlation between
30 reworked coccoliths and the N-Ratio ($r=-0.44$; $p=6^{-7}$) suggest that fresh water induced
31 stratification is a controlling factor of the SAS coccolithophorid production. High
32 coccolithophorid productivity levels occurred during dry periods and/or time intervals of
33 inflowing salty and nutrient-rich Levantine Intermediate Waters (LIW) favouring convection
34 while lower levels took place during high freshwater discharge, mainly during the Little Ice
35 Age (LIA) and two centennial scale intervals of weakest NAO around 200 BCE and 500 CE.

36

37 **Keywords**

38 Coccolithophores; reworked coccoliths; coccolithophorid primary productivity; South
39 Adriatic Sea; central Mediterranean; last millennia.

40

41

42 **Introduction**

43 Coccolithophores (calcareous nanoplankton) and their fossil remains (calcareous
44 nannofossils) are valuable source of information for paleoclimatic studies (Baumann et al.,
45 2005). Coccolithophores are single cell calcareous algae whose ecology and vital functions
46 are driven by environmental parameters within the ocean euphotic zone (e.g., temperature,
47 salinity, sunlight, and nutrient supply). Therefore, abundances of selected taxa have been used
48 to reconstruct variations of physical and environmental parameters and their relation with
49 climate change and human activity. Their skeletons composed of tiny calcareous platelets
50 (coccoliths) are highly abundant in marine sediments making them ideal fossils to produce
51 high-resolution time series (Baumann et al., 2005). These microorganisms are usually
52 considered to prefer warm, stratified, oligotrophic waters of low and middle latitude regions
53 (e.g., Honjo and Okada, 1974; Ziveri et al., 2004). However, local oceanic features such as
54 coastal currents, gyres, eddies, upwelling, and river runoff are known to regionally affect their
55 productivity (Guerreiro et al., 2013). In addition, reworked coccoliths (i.e., the nannofossils
56 which have been removed from their original sedimentary layer and redeposited in a younger
57 layer) can provide information on sediment transport (Bonomo et al., 2014; Ferreira et al.,
58 2008; Ferreira and Cachão, 2005) and used to reconstruct regional scale runoff and/or
59 precipitation changes (Bonomo et al., 2016a; Incarbona et al., 2010; Sprovieri et al., 2006).

60 Understanding the trends and variability of the Mediterranean climate at local and regional
61 scales has been subject of intense research. (Bonomo et al., 2016a; Cacho et al., 1999; Frigola
62 et al., 2007; Martrat et al., 2004; Pérez-Folgado et al., 2004; Rodrigo-Gámiz et al., 2011;
63 Rohling et al., 2002, 2015; Sbaiffi et al., 2001; Sierro et al., 2005; Sprovieri et al., 2003, 2006;
64 Triantaphyllou et al., 2009, 2016a). Shelf sediments of the Adriatic Sea (AS) provide ideal
65 natural archives for high-resolution paleoclimatic investigations because of expanded
66 Holocene sedimentary sequences and possible use of recurrent tephras for geochronological

67 control (Jalali et al., 2018; Lowe et al., 2007; Marchini et al., 2014; Matthews et al., 2015;
68 Siani et al., 2013). Terrestrial and marine paleoclimate proxy data (e.g., calcareous plankton,
69 lipid biomarkers, palynomorphs, stable isotopes, lake levels, and speleothems) have shown
70 the occurrence of abrupt climate changes during the Holocene (warmer/colder and
71 drier/wetter periods) at decadal, centennial to millennial time scales in the Mediterranean
72 basin (e.g., Bini et al., 2019; Cisneros et al., 2016; Di Bella et al., 2014; Gogou et al., 2016;
73 Goudeau et al., 2015; Grauel et al., 2013; Jalali et al., 2016, 2018; Kouli et al., 2012; Lirer et
74 al., 2013, 2014; Margaritelli et al., 2016, 2018; Piva et al., 2008; Sicre et al., 2016; Skampa et
75 al., 2019; Triantaphyllou et al., 2009, 2010, 2016b).

76 Many studies have focussed on (late) Holocene climate variability and its impact on the
77 environment and human activity in the SAS (Caroli and Caldara, 2007; Combourieu-Nebout
78 et al., 2013; Di Rita and Magri, 2009; Giunta et al., 2003; Grauel and Bernasconi, 2010; Jalali
79 et al., 2018; Leider et al., 2010; Oldfield et al., 2003; Piva et al., 2008; Sangiorgi et al., 2003;
80 Siani et al., 2013; Sicre et al., 2016). The recent study of Jalali et al. (2018) in the SAS
81 highlighted the links between the centennial scale variability of SSTs and local climatic and
82 oceanographic features, and notably the role of the Bimodal Oscillating System (BiOS) of the
83 Ionian Sea and North Atlantic Oscillation (NAO). Although there has been a substantial
84 number of publications on the investigated area, very few studies have explored calcareous
85 nannofossils as a proxy of past climate and environmental changes (e.g., Giunta et al., 2003;
86 Narciso et al., 2012; Sangiorgi et al., 2003). Narciso et al. (2012) studied a gravity core close
87 to our site between 13000 and 5500 BP, thus focused on the Greenland Stadial 1/Younger
88 Dryas, Pre-Boreal, and Sapropel 1 equivalent periods. Giunta et al. (2003) and Sangiorgi et al.
89 (2003) reported data from 18000 to 2300 yrs BP at a more southern site, documenting the
90 distribution of calcareous nannofossils during the Sapropel S1. As far as living
91 coccolithophores are concerned, the only study carried out in the SAS is that of Balestra et al.
92 (2008) describing assemblages in the water column and surface coastal sediments of the Gulf

93 of Manfredonia (SAS). Other very recent data were restricted to the Mid and North Adriatic
94 Sea (e.g., Cerino et al., 2017; Godrijan et al., 2018; Skeji et al., 2018, and references there
95 in) or are part of phytoplankton biomass and productivity assessments aiming at providing
96 rough estimates of coccolithophore distribution in open SAS (e.g., Fonda Umani, 1996;
97 Ljubimir et al., 2017, and references therein).

98 The aim of this work is to evaluate the reliability of Coccolithophores/calcareous nannofossils
99 as a proxy of environment and climate variability over the last three millennia in the Central
100 Mediterranean. For this purpose, we carried out a high-resolution study from a deep-sea
101 gravity core recovered in the SAS and from a second shallow coastal gravity core (C5
102 Composite) from the Tyrrhenian Sea (Gulf of Gaeta) obtained within the framework of the
103 NEXTDATA Project (<http://www.nextdataproject.it>). Our data evidence major changes in
104 nutricline depth as well as variations of river runoff and precipitation. We explore the cause of
105 the observed changes by comparing our results to alkenone derived Sea Surface Temperatures
106 (SSTs) and terrestrial inputs derived from higher plant biomarkers (Jalali et al., 2018). We
107 also use other indicators of past precipitation changes in the Mediterranean basin: i.e. the
108 flood activity in the Southern Alps (Wirth et al., 2013), the reworked coccolith record from a
109 Southern Tyrrhenian sea core (Bonomo et al., 2016b), the XRF record from lake sediments of
110 the Iberian Peninsula (Moreno et al., 2012) and the reconstruction of the forested fraction of
111 usable land in Central and Western Europe (Kaplan et al., 2009).

112

113 **Oceanographic setting of the study area**

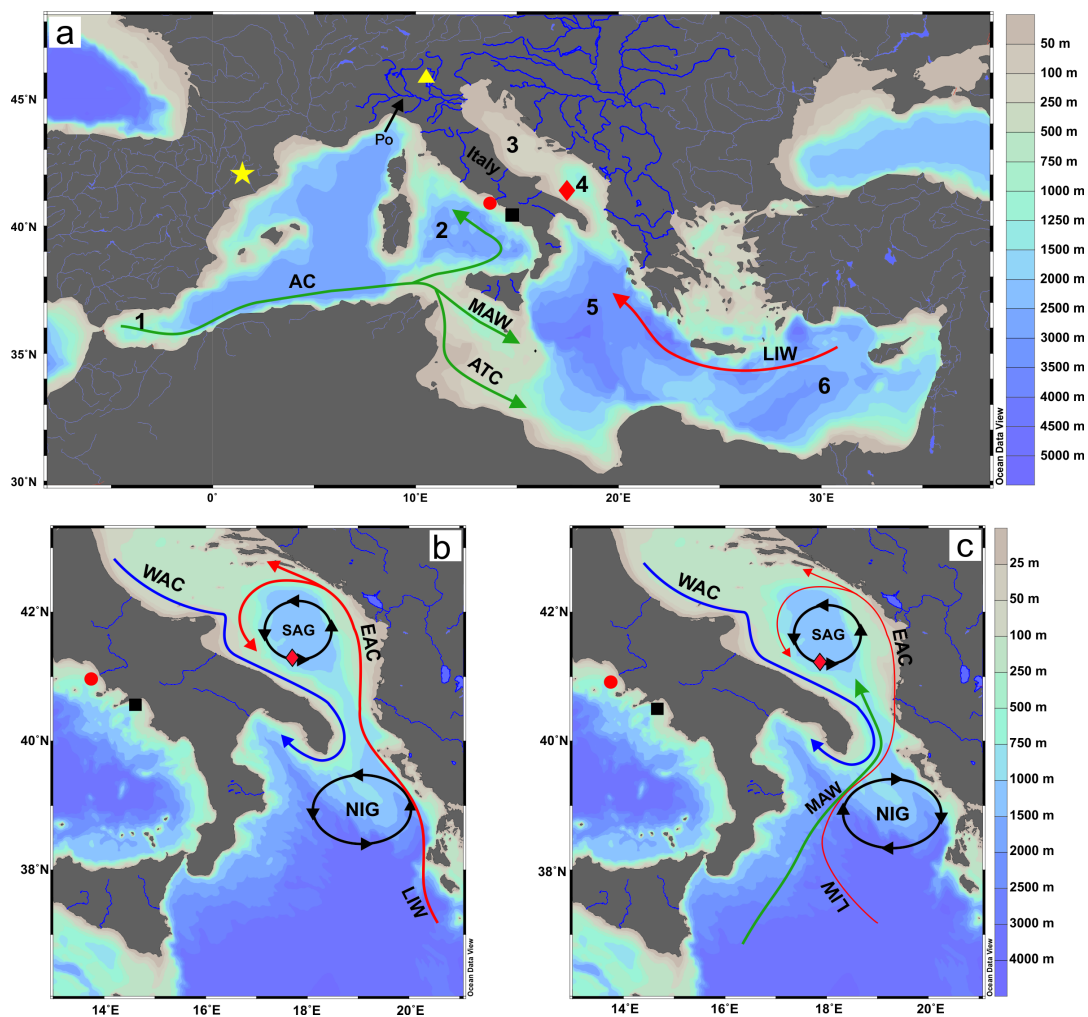
114 The AS is a semi-enclosed basin located between the Italian Peninsula and the Balkans,
115 connected to the Mediterranean Sea through the Strait of Otranto (Fig.1a). The North Adriatic
116 (NA) is primarily influenced by the southeast Europe climate, while the SAS experiences
117 more arid conditions typical of Mediterranean and Northern Africa climates (Ilijani et al.,
118 2014). The general surface circulation of the AS is cyclonic (Fig.1b,c) (Sellschopp and

119 Álvarez, 2003) and consists of a northward current flowing along the eastern Adriatic coast
120 (i.e., the Eastern Adriatic Current, EAC) balanced by southward current flowing along the
121 western coast (i.e., the Western Adriatic Current, WAC). The intermediate layer mainly
122 present in the southern and mid AS is occupied by the Levantine Intermediate Water (LIW)
123 (Artegiani et al., 1997). The deep circulation is characterized by the Adriatic Deep Water
124 (ADW) a dense water mass formed by the mixing of the Northern Adriatic Dense Water
125 (NADW) and Southern Adriatic Dense Water (SADW) (Manca et al., 2002).

126 The SAS is a sub-basin (South Adriatic Pit, SAP, 1260 m max depth) characterized by a
127 quasi-permanent cyclonic circulation, i.e. the South Adriatic Gyre (SAG; Ga i et al., 1997)
128 (Fig. 1b,c). The physical and chemical properties of SAS surface waters depend on the
129 characteristics of inflowing waters into the basin, the strength of SAG, as well as wind stress
130 and river discharges. Inflowing waters consist mainly of WAC and NADW from the North,
131 the LIW and occasionally Modified Atlantic Water (MAW) from the South. The WAC is
132 strongly influenced by river runoff mostly from the Po River, making it fresher and nutrient
133 rich. The inflow of LIW and MAW depends on the variability of the North Ionian Gyre (NIG)
134 (Fig. 1b,c). According to the BiOS (Bimodal Oscillating System) model, the NIG circulation
135 may either be cyclonic or anticyclonic (Civitarese et al., 2010; Gacic et al., 2010). This
136 mechanism is sustained by internal processes driven by the density of the ADW outflowing
137 the Otranto Strait. When the circulation in the NIG is cyclonic, saltier and warmer LIW enters
138 the SAS promoting deep convection and the formation of a denser ADW. In an anticyclonic
139 NIG mode, fresher and colder MAW enters the SAS leading to the production of lower
140 density ADW. However, some studies invoke the role of more complex driving mechanisms
141 involving the whole Ionian Sea circulation and not just its northern sector (Reale et al., 2016;
142 Simoncelli et al., 2016; Theocharis et al., 2014). The intensity of the SAG depends on local
143 wind intensity and properties of advected waters from the Ionian Sea (Shabrang et al., 2016).
144 Shabrang et al. (2016) reported a significant negative correlation between the NAO index and

145 local wind intensity. However, they did not find unequivocal relationship between the NAO
 146 and SAG variability because of additional effects of the advection of the Ionian waters,
 147 suggesting that the BiOS mode does not depend on NAO. Nevertheless, Pinardi et al. (2015)
 148 reported a sustained BiOS anticyclonic circulation during the period of positive NAO in
 149 1987-1996.

150 The surface waters of the SAS are more oligotrophic than those of the NA (e.g., Civitarese et
 151 al., 1998). The influence of Po River and secondary Apennines rivers flowing into the western
 152 AS on the nutrient budget of the SAS seems rather weak and limited to a narrow coastal
 153 current flowing over the Italian shelf (Faganeli et al., 1989). The nutrient supply to the SAS
 154 occurs mainly via the inflow of LIW lying at about 300 m in the Adriatic Sea (Gai et al.,
 155 2002). Nevertheless, according to Civitarese et al. (2010) larger amounts of nutrients are
 156 advected by the MAW during periods of anticyclonic BIOS.



157

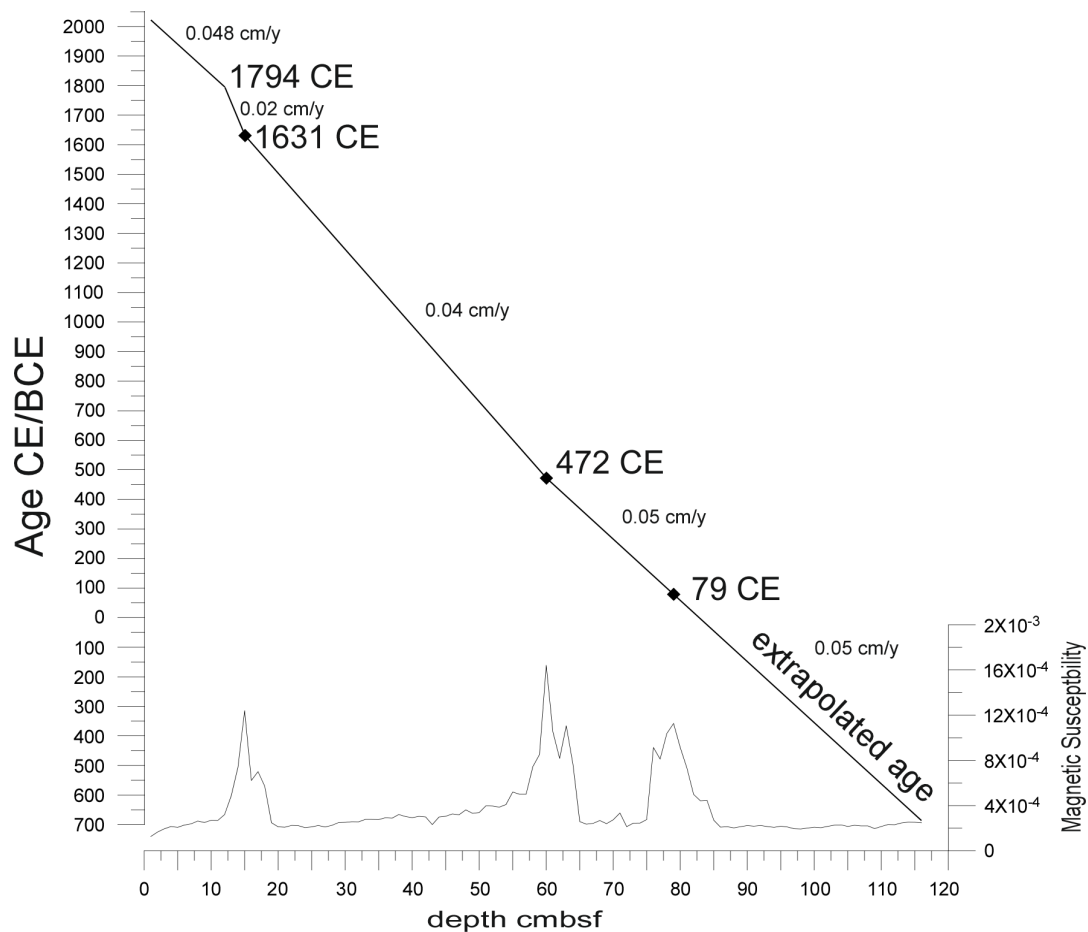
158 **Figure 1.** Location of the cores SW104-ND14Q (diamond), C5 Composite (dot), C90 (square,
159 Lirer et al., 2013), Basa de la Mora (star, Moreno et al., 2012), and Ledro (triangle, Wirth et
160 al., 2013). (a): bathymetric map of the Mediterranean Basin and main surface (green arrow)
161 and intermediate circulation pattern (red arrow). AC: Algerian Current; MAW: Modified
162 Atlantic Water ; ATC: Atlantic Tunisian Current; LIW: Levantine Intermediate Water.
163 Numbers 1-6: 1-Alboran Sea; 2-Tyrrhenian Sea; 3-Adriatic Sea; 4-South Adriatic Pit, SAP; 5-
164 Ionian Sea; 6 Levantine Sea. The main catchment basins of river flowing into the Adriatic Sea
165 are reported (blue thick lines). (b) and (c): bathymetric map and main circulation pattern of
166 South Adriatic Sea and North Ionian Sea during cyclonic (b) and anticyclonic (c) mode of the
167 BiOS; WAC: Western Adriatic Current; EAC: Eastern Adriatic Water; LIW: Levantine
168 Intermediate Water; MAW: Modified Atlantic Water; SAG: South Adriatic Gyre; NIG: North
169 Ionian Gyre.

170

171 **Methods**

172 *Core SW104-ND14Q*

173 Core SW104-ND14Q (17°37'3.612''E; 41°17'2.4''N) was recovered at 1013m water depth in
174 the SAS (Fig. 1). The sedimentary sequence was retrieved with a SW104 gravity corer
175 system, which preserves the water-sediment interface and allowed the recovery of 116 cm of
176 undisturbed and uncompressed homogeneous brown-grey hemipelagic sediments. The
177 magnetic susceptibility measured on board with a Bartington Instrument M2 revealed three
178 tephra layers (Fig. 2). The age model used here is from Jalali et al. (2018) and has been
179 constructed combining radionuclides ages (^{210}Pb activity-depth profile and ^{137}Cs activity) for
180 the last ca. 150 years and the additional dates derived from the correlation of three tephra
181 layers with well-dated volcanic events onland [Pompeii eruption (79 CE); Pollena eruption
182 (472 CE); 1631 CE] (see Jalali et al. 2018 for details on tephrostratigraphy). Linear
183 interpolation between the tie-points has been used to construct the age-depth profile from the
184 top down to the base core documenting a mean Sed. Rate of 0.04 cm/y (Fig. 2). Based on the
185 age model, core SW104-ND14Q ranges from 700 BCE to 2003 CE and has a mean temporal
186 resolution of ~26 yrs.



187

188 **Figure 2.** SW104-ND14Q age-depth model and magnetic susceptibility signal. Sedimentation
 189 rate and tephra layers (diamond) were reported.

190

191 *Core C5 Composite*

192 To investigate the reliability of the reworked coccoliths as a regional proxy of precipitation,

193 we also used the central Tyrrhenian Sea shallow sequence C5 Composite (C5Comp) (Fig.1).

194 The location of this site in front of Volturno River mouth makes it particularly suitable for

195 reconstructing runoff variability and for comparing coastal and open sea sites (Bonomo et al.,

196 2016). The core C5Comp is a composite marine sequence consisting of two cores: the

197 SW104-C5 and core C5 (710 cmbsf length) both recovered in the Gulf of Gaeta, at 93 m

198 water depth (see Margaritelli et al., 2016 for details). Calcareous nannofossils of the core

199 SW104-C5 (back to 1630 CE) was already published by Bonomo et al. (2016). In this work

200 we extended their reconstruction back to ~ 400 CE. The chronology used is that of

201 Margaritelli et al. (2016) and has been assembled combining radionuclides ages (^{210}Pb

202 activity-depth profile and ^{137}Cs activity) for the last ca. 150 years, planktonic foraminiferal

203 event, tephrostratigraphy and oxygen stable isotope correlation with other marine sites (for
204 details see Margeritelli et al., 2016). The age-depth profile has been constructed by a linear
205 interpolation between the tie-points showing a progressive decrease in sedimentation rate
206 from the top down to the base core.

207 The analysed time interval of core C5Comp covers the period between ~ 400 and 2013 CE
208 with a mean temporal resolution of ~10 yrs.

209 *Calcareous Nannofossils*

210 116 samples of the SW104-ND14Q core and 108 of the C5Comp were prepared as standard
211 smear slides (Bown, 1998) and analyzed with a transmitted light microscope at x1250
212 magnification. Some samples of SW104-ND14Q core were analysed with a scanning electron
213 microscope (SEM) in order to solve taxonomic identification for smaller placoliths difficult to
214 achieve by light microscope (e.g., *Emiliania huxleyi*). The relative abundance of *in situ*
215 species was estimated only in the SW104-ND14Q core based on the count of at least 600
216 specimens. The abundance of reworked nannofossils was estimated in the SW104-ND14Q
217 and C5Comp as the number of reworked specimens encountered during the count of the *in*
218 *situ* coccoliths. All abundances are expressed in percentages. SW104-ND14Q coccolith
219 species abundances were also used to calculate the N-ratio as defined by Flores et al. (2000)
220 to assess the nutricline depth fluctuations. The N-ratio is based on the absolute abundances of
221 the main surface r-strategist species (in our record *E. huxleyi* and small placoliths) over that of
222 *F. profunda* (lower photic zone taxon). High values of the N-ratio indicate shallow
223 nutricline/thermocline (relatively high surface coccolithophorid productivity) while low
224 values indicate deep nutricline/thermocline (relatively low surface coccolithophorid
225 productivity). As small placoliths, we counted the placoliths not confidently recognizable as
226 *E. huxleyi* and *Reticulofenestra* spp.

227 Finally, the reworked coccoliths (RC) group includes taxa from different stratigraphic
228 intervals (Mesozoic, early Cenozoic) and Cenozoic long-range taxa showing poor
229 preservation (etching and/or overgrowth). Raw data are shown in supplementary material.

230

231 *Ecology of selected taxa*

232 *E. huxleyi* tolerates a wide range of ecological conditions and is therefore abundant in nearly
233 all oceanic environments (Schwab et al., 2012). This species is considered an opportunistic (r-
234 strategist) taxon capable to quickly respond to nutrient availability in both eutrophic and
235 oligotrophic areas (e.g., Balestra et al., 2008; Broerse et al., 2000; Dimiza et al., 2008, 2015;
236 Haidar and Thierstein, 2001). *E. huxleyi* is generally more abundant in temperate (cold) mixed
237 surface waters (e.g., Hagino et al., 2000; Malinverno et al., 2003), but may also be found in
238 stable regimes in terms of vertical mixing with relatively high nutrient availability (Andruleit
239 et al., 2005). Ausín et al. (2015) further postulated that *E. huxleyi* (size >4 µm) can find
240 optimal conditions for its development in cold water that are also low-salinity.

241 The lower photic zone species *F. profunda* has a more constrained habitat and has thus been
242 widely used to monitor past changes in nutricline-depth and induced changes in surface
243 productivity (Beaufort, 1997). The abundance of *F. profunda* increases with respect to other
244 coccolithophores when the nutricline is deep and overlaid by a nutrient-depleted upper photic
245 layer (Balestra et al., 2008; Bown et al., 2009; Dimiza et al., 2015; Incarbona et al., 2008,
246 2010). These conditions generally reveal stable, stratified, oligotrophic surface waters during
247 summer months (Baumann et al., 2005; Malinverno et al., 2009) that can be disrupted under
248 increased wind stress and / or upwelling and divergence circulation (Bown et al., 2009).
249 Hernández-Almeida et al. (2019), using *F. profunda* relative abundance vs MODIS (Moderate
250 Resolution Imaging Spectroradiometer) chlorophyll- α , show a pronounced temperature
251 sensitivity of *F. profunda* and no correlation with surface net primary production at latitudes
252 higher than 30°N–30°S, such as Mediterranean area. Contrary, Grelaud et al. (2012) showed a

253 strong anticorrelation ($R = -0.76$) between *F. profunda* % and chlorophyll- α in the Aegean
254 Sea (eastern Mediterranean Sea).

255 *Biomarker analyses*

256 Sea surface temperature and TERR-alkane reconstructions along the SW104-ND14Q core
257 have been published by Jalali et al (2018). The method used for biomarker analyses have been
258 described by (Sicre et al., 2002). Fatty alcohol biomarker data were used to calculate the C_{26}
259 fatty alcohol / C_{29} n-alkane + C_{26} fatty alcohol ratio ($C_{26OH}/(C_{26OH}+C_{29})$). This ratio was
260 determined along the core to infer information on water oxygenation as proposed by Cacho et
261 al. (2000). High values of this ratio presumably correspond to low ventilation and *vice versa*.

262

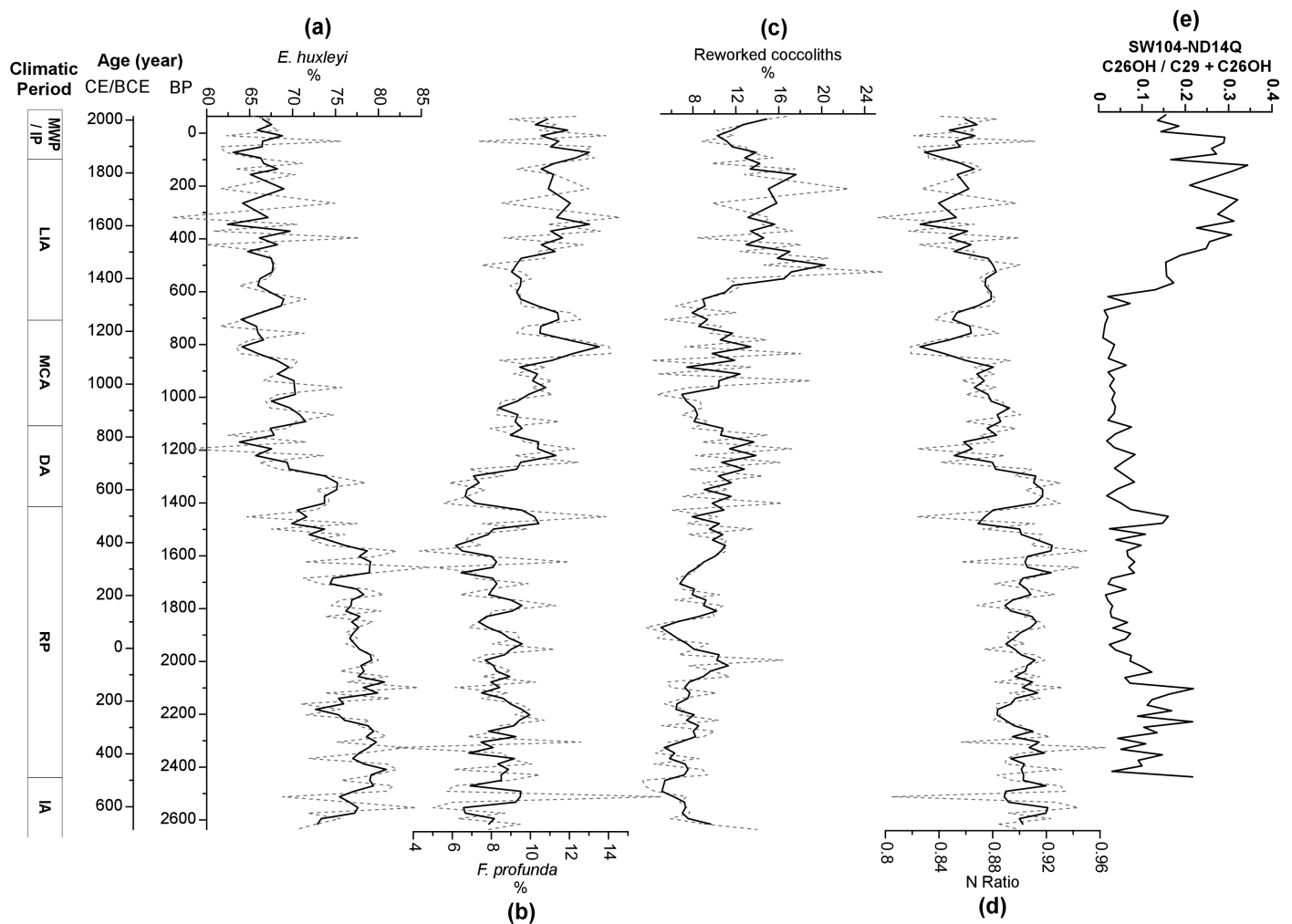
263 **Results**

264 The coccolithophore assemblages in the SW104-ND14Q core are generally well preserved
265 and abundant. *E. huxleyi* dominates the assemblages with an average abundance of ~80%. *F.*
266 *profunda* is also well represented with an average abundance of ~10%. Other taxa are largely
267 subordinated with percentages ranging between ~1- 3% (e.g. *Syracosphaera*, *Rhabdosphaera*
268 and *Calciosolenia*) and no significant variations (not shown). Reworked specimens are always
269 present and are found in higher amounts in the upper part of the core. *E. huxleyi*, *F. profunda*,
270 RC, and the N-ratio data shown in Figure 3 are used for the discussion.

271 *E. huxleyi* abundance range from 65 to 90 % (Fig. 3a). Its downcore distribution pattern can
272 be divided into two major intervals. A first one that includes the late Iron Age (IA) and the
273 almost entire Roman Period (RP; between ~700 BCE and ~400 CE) with abundance above
274 80%. This period is followed by a decline to lower values (< 65%) between ~400 and ~800
275 CE, i.e. from the late RP throughout the Dark Age (DA). *E. huxleyi* returns to moderately
276 higher abundances (65 - 75%) at the late DA and during the Medieval Climate Anomaly
277 (MCA) (800 to 1100 CE). Then, values remain approximately at these levels but with
278 superimposed short-lived oscillations especially during the upper LIA. The distribution of *F.*

279 *profunda* (Fig. 3b) reveals three main intervals: the first one runs from the bottom of the core
280 till ~400 CE and is characterized by fluctuating values between 7 and 9 %. Over the second
281 interval, from 400 to 1200 CE, the taxon abundances increase almost continuously, except for
282 two time spans of strong decrease centred at 600 and 900 CE. From 1200 CE, *F. profunda*
283 declines till 1550 CE and rises again to Present day values. As shown in Fig. 3d, the N-ratio
284 shows similar trends as *E. huxleyi*, but with more pronounced fluctuations especially in the
285 upper half of the core. During the first 1200 years (700 BCE - 400 CE) the N-ratio value is >
286 0.9. At ~400 CE a sharp drop sets the beginning of a long-term decreasing trend till Present
287 that suggests a progressive reduction of coccolithophorid productivity.

288 RC percentages (%RC) along the core range from ~3 to ~25%, and depict a steady increase
289 from the bottom core to ~800 CE. Then, after a period of lower values around 900 CE and
290 1300 CE, %RC increases up to Present with the highest values (17-25%) during the LIA
291 (~1400 -1800 CE) (Fig. 3c). In the C5Comp core, %RC ranges from ~14 to ~79% with lowest
292 levels found between ~400 and ~1350 CE.



294 **Figure 3.** Time domain distribution of (a) *E. huxleyi*, (b) *F. profunda*, (c) RC, (d) N-ratio, and
 295 (e) $C_{26OH}/C_{29}+C_{26OH}$ ratio in core SW104-ND14Q. Raw and three points running average data
 296 are reported in grey dashed and black full lines, respectively. The age model is from Jalali et
 297 al. (2018) and the climate period intervals are those of Margaritelli et al. (2016).
 298

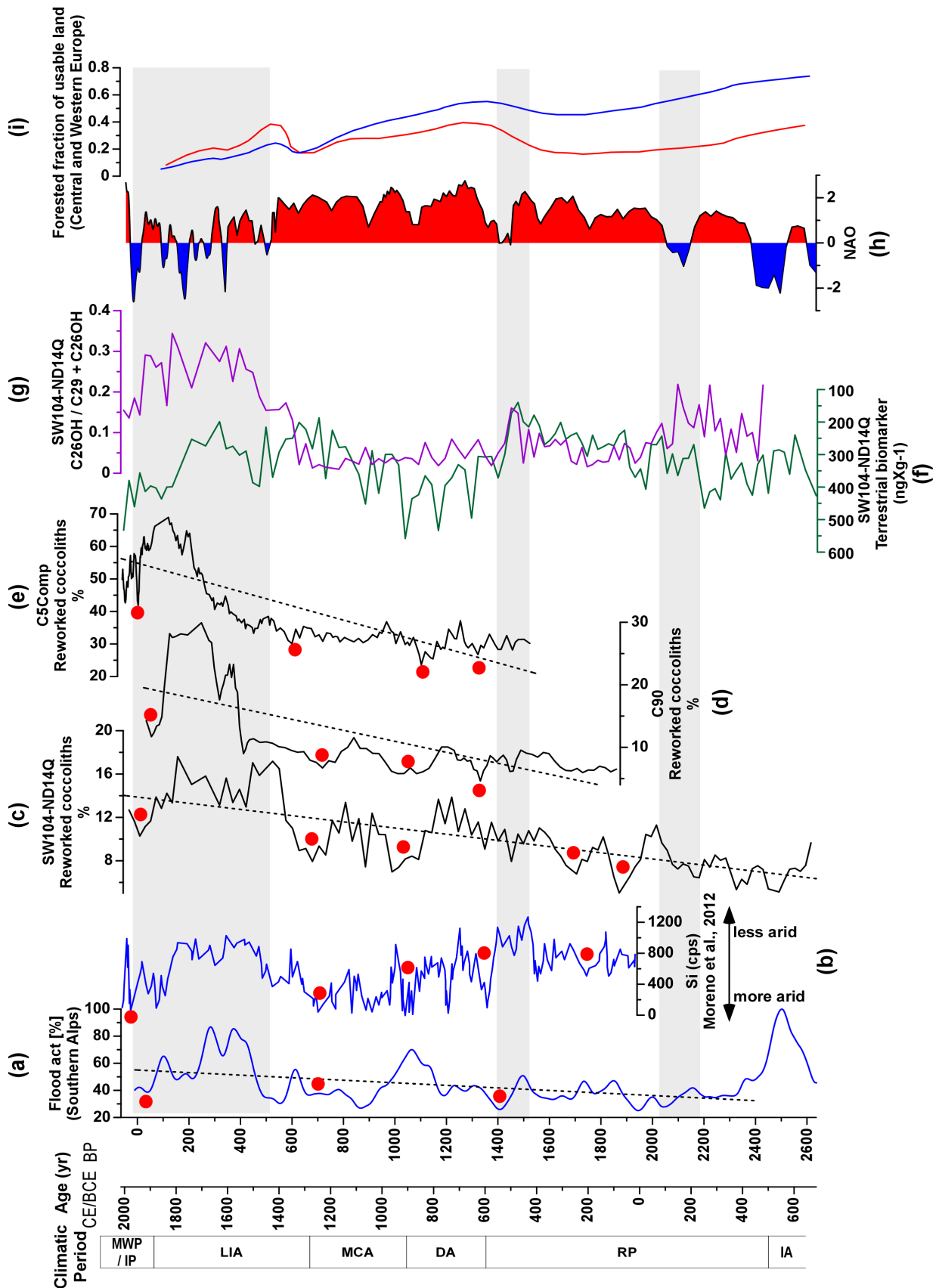
299 Discussion

300 *Reworked coccoliths and runoff fluctuations*

301 The NAO is one of the dominant atmospheric mode of variability in the North Atlantic sector
 302 that has a considerable influence on winter temperature/precipitation in Europe including the
 303 Mediterranean region (Hurrell, 1995). In the central Mediterranean, positive NAO conditions
 304 result in colder and drier winters than average, while winters are warmer and wetter during
 305 negative phases of NAO (Benito et al., 2015; López-Moreno et al., 2011a, 2011b; and
 306 references within). Bonomo et al. (2016) were able to evidence a negative correlation between
 307 the NAO index of Trouet et al. (2009) and the %RC in the Central Tyrrhenian Sea core

308 SW104-C5 over the last 400 years. Our results show that this relationship could have
309 persisted back to ~700 BCE (Fig. 4). The resemblance between the %RC short and long term
310 trends the flood frequency in Southern Alps (Wirth et al., 2013) and the Southern Tyrrhenian
311 marine record (Gulf of Salerno; Lirer et al. 2013) seems to confirm the link between the %RC
312 and runoff/precipitation in the region on longer time span (Bonomo et al., 2016a; Incarbona et
313 al., 2010; Sprovieri et al., 2006). This finding is supported by the slight negative correlation
314 between the NAO index of Trouet et al. (2009) ($r=-0.4$ $p=5^{-33}$, $n=34$) and Olsen et al. (2012)
315 ($r=-0.2$ $p=0.01$, $n=82$) and the %RC along the SW104 record. Our data agree with the
316 negative correlation between NAO and winter precipitation, for the 1950–2006 period,
317 reconstructed over large areas of Morocco and Tunisia, most of the Iberian Peninsula,
318 southeastern France, Italy, the Balkan Peninsula, and large areas of central and northern
319 Turkey (López-Moreno et al., 2011a). Notwithstanding the age models accuracy of the
320 different cores, the main drier spells recorded in the SAS, in the Central and Southern
321 Tyrrhenian as shown by red dots in Fig. 4 might be considered synchronous as well to the
322 XRF Si fluctuations found in lake sediments of Iberian Peninsula (Moreno et al., 2012). A
323 noteworthy result is the high %RC (RC Acme event) during the late LIA, between ~1600 and
324 ~1850 CE, that coincides with a long standing interval of negative NAO and is consistent
325 with a regional scale humid period already documented in marine and continental sedimentary
326 sequences of the Western and Central Mediterranean (e.g., Barrera-Escoda and Llasat, 2015;
327 Goudeau et al., 2015; Vallefucio et al., 2012; Moreno et al. 2012) .
328 Jalali et al. (2018) highlighted similarities between the TERR–alkane record in SW104-
329 ND14Q and the forested fraction of usable land (FF) in Central and Western Europe (Fig.4 f,
330 i) (Kaplan et al., 2009). Considering that FF fluctuations are indicative of anthropogenic
331 deforestation (Kaplan et al., 2009), they concluded that TERR–alkane at SW104-ND14Q
332 reflects primarily human activity rather than climate fluctuations. Since the RC signal does
333 not match with either the TERR–alkanes or FF index but with the flood activity

334 reconstruction and the $C_{26OH}/(C_{26OH}+C_{29})$ ratio (Fig.4), we suggest that RC reflect
 335 precipitation changes that are also seen in other Mediterranean RC records overall supporting
 336 the hypothesis that %RC is a reliable index of past runoff/precipitation changes in the region.



337

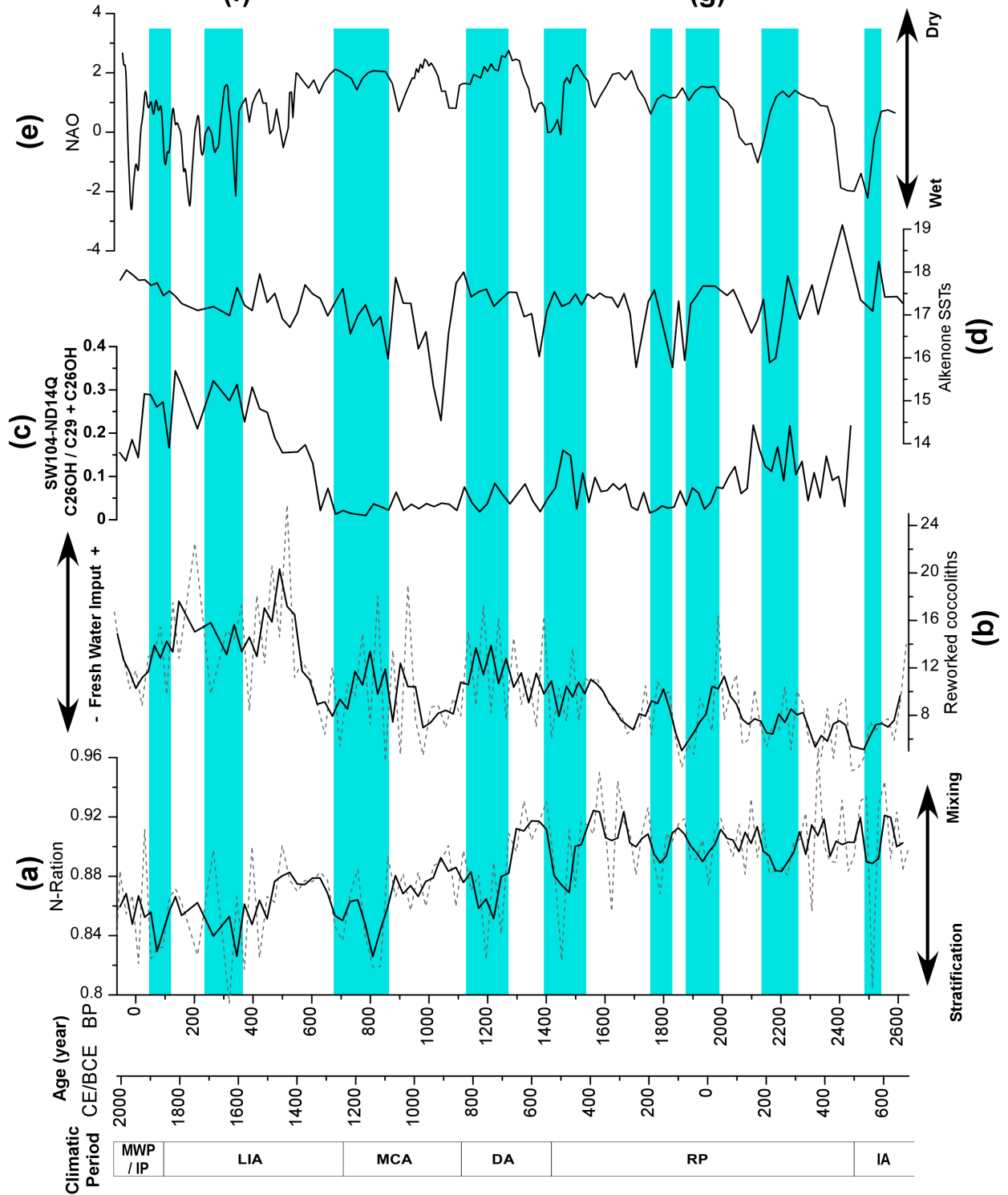
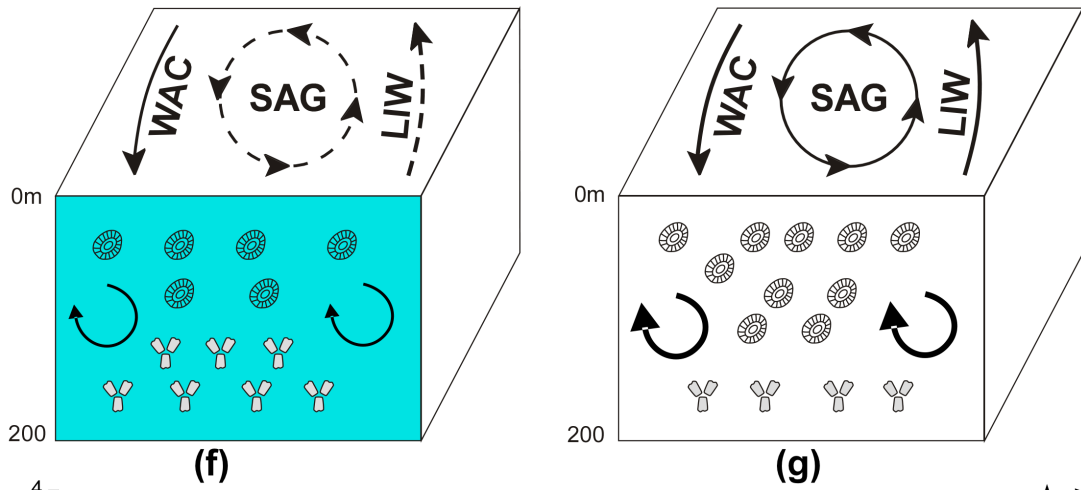
338 **Figure 4.** Comparison in time domain between (c) SW104-ND14Q, (d) C90, and (e) C5Comp
339 reworked coccoliths, (g) SW104-ND14Q $C_{26OH}/C_{29}+C_{26OH}$ ratio, (b) Si fluctuations (Moreno
340 et al., 2012), and (a) Flood frequency reconstruction from Southern Alps (Wirth et al., 2013).
341 (f) Terrestrial biomarker concentration (Jalali et al., 2018) and (i) Forest fraction of usable
342 land (Kaplan et al., 2009) are reported. The dots mark the dry spells identified in the records.
343 The bands highlight the relationship between $C_{26OH}/C_{29}+C_{26OH}$ ratio and negative (h) NAO
344 states. The climate periods are from Margaritelli et al. (2016).
345

346 *N-ratio and South Adriatic hydrology*

347 Highest N-ratio values almost all along the RP indicate shallow nutricline (surface productive
348 waters) during this period considered as generally mild (Figs. 3, 5). This is in contrast with
349 the LIA showing deep nutricline (lower surface productivity levels) (Figs. 3, 5), a cold period
350 that one would expect to be favourable to water column mixing and growth of r-strategy taxa
351 *E. huxleyi*. Comparable results has been recorded in the North Aegean Sea during the last
352 1500 years (Gogou et al., 2016; Skampa et al., 2019). In particularly, in the North Aegean Sea
353 Gogou et al.(2016) and Skampa et al. (2019) recorded periodic occurrence of “*E. huxleyi*
354 dominance” intervals indicating strong water column convection coupled with NAO positive
355 shifts , EMT-like events (Incarbona et al., 2016), cool spells, and enhanced continental inputs
356 as well. In contrast, the occurrence of *F. profunda* dominance intervals may be linked to
357 enhanced stratification of the upper water column and warm surface waters, potentially
358 associated with increased lower salinity Black Sea Water intrusion. During the RP, alkenone-
359 derived SSTs show cold oscillations that do not seem to have any relationship with the N-
360 ratio (Fig. 5 a, d). Local atmospheric and hydrological conditions (i.e. properties of inflowing
361 waters into the basin and strength of SAG) play an important role in the stratification of the
362 upper water column and associated changes in productivity (Civitaresse et al., 2010; Ljubimir
363 et al., 2017; Vilibi et al., 2012). Several studies in open sea SAS waters have linked high
364 abundances of coccolithophorids with the inflow of saltier Ionian waters (Fonda Umani,
365 1996; Totti et al., 2000). In contrast, Ljubimir et al. (2017) reported higher abundances of
366 coccolithophorids in lower salinity SAG waters during years of anticyclonic mode of the

367 BIOS and their absence during cyclonic BIOS years. However, despite the lack of significant
368 correlation between salinity and total coccolithophore abundances, increased abundance of *E.*
369 *huxleyi* has been often related to the inflow of LIW or eastern Mediterranean surface waters
370 (Malinverno et al., 2003; Skeji et al., 2018). Advection of saltier LIW by promoting deep
371 convection (Gai et al., 2014) would favour the development of *E. huxleyi* known to rapidly
372 respond to increased nutrient supply to the photic zone (Fig.5 g) (Malinverno et al., 2003).
373 Conversely, reduced inflow of LIW, or enhanced input of less salty waters (mainly the WAC,
374 and occasionally the MAW), and a weak SAG, would lead to higher surface water buoyancy
375 and stratified conditions (Fig.5 f, g). The consequent deepening of the nutricline would thus
376 favour *F. profunda* growth (Fig. 5 f). This conceptual scheme is in agreement with the slight
377 negative correlation ($r = -0.44$; $p = 6^{-7}$) between the N-ratio and %RC values. For instance,
378 higher values of %RC associated with sustained negative NAO during the LIA are coherent
379 with higher precipitation and runoff (Bonomo et al., 2016a; Incarbona et al., 2010; Sprovieri
380 et al., 2006) and the Po River flood record (Camuffo and Enzi, 1996). Rising
381 $C_{26OH}/(C_{26OH}+C_{29})$ ratio to their highest values suggests an abrupt reduction of water
382 oxygenation that is also compatible with stratified conditions caused by the large freshwater
383 discharge during the LIA and lowest N-ratios. Similar observation can be made for two
384 intervals of weaker NAO, i.e. around 200 BCE and around 500 CE.
385 Regarding nutrient supply, our results also support the idea of a limited influence of the Po
386 River (and secondary Apennines rivers) on the nutrient budget of the open SAS surface
387 waters and coccolithophore productivity, as the nutrients are usually rapidly consumed during
388 their transport within the WAC. The same have been observed around the eastern Adriatic
389 coasts (Vilibi et al., 2012). Overall, our findings suggest that fresh water input due to
390 increased precipitation and river runoff impact essentially on buoyancy and subsequent
391 stratification in the SAG.

392 Apart from the LIA and these two major short time intervals that all took place during
393 prolonged negative NAO, other N-ratio fluctuations cannot robustly be attributed to NAO and
394 high river discharge (Fig. 5). Under weaker freshwater forcing, other factors such as the BIOS
395 circulation may have been a more important controlling factor on the SAG dynamics and
396 productivity, but this question will need further investigations to be addressed.



398 **Figure 5.** Schematic view of inferred relationship between (a) SW104-ND14Q N-Ratio and
399 (f, g) SAS hydrology. (b) %RC fluctuations, (c) $C_{26OH}/C_{29}+C_{26OH}$ ratio, (d) SSTs fluctuations,
400 and (e) winter NAO index (Olsen et al., 2012; Trouet et al., 2009) are reported. The bands
401 highlight the N-Ratio during periods of stratified surface water (diagram f). The climate
402 periods are from Margaritelli et al. (2016).

403

404 **Conclusion**

405 This high-resolution study of calcareous nannofossils from the sediment core SW104-ND14Q
406 was used to provide information on paleoceanographic and climatic conditions in the SAS,
407 over the past ~2700 years. Based on the distribution of *E. huxleyi*, *F. profunda*, the N-ratio,
408 and reworked coccoliths we were able to evidence hydrological variability and related
409 coccolithophore production changes in the SAG.

410 One outstanding result is the good correspondence we found between the % reworked
411 coccoliths in the SAS and Tyrrhenian Sea cores and flood activity across the Southern Alps,
412 highlighting the value of %RC as a proxy for reconstructing regional scale precipitation and
413 runoff.

414 We also showed that lowest N-ratio took place during extended weakest NAO phases, i.e.
415 primarily the LIA and two other intervals (200BCE and 500CE), as a result of large fresh
416 water discharge and subsequent stratified surface ocean reducing nutrient supply and
417 production of coccolithophorids in the SAG. Outside these periods of strong negative NAO,
418 whether and to what extent other factors such as the BIOS may have played a role on the
419 hydrology and productivity of the SAG remains an open question.

420

421 **Acknowledgments**

422 We would like to thank the two anonymous reviewers for their useful and constructive
423 comments. The core SW104-ND14Q has been collected by ISMAR-CNR (Napoli) aboard of
424 the R/V-Urania during the oceanographic cruise NEXTADATA2014. This research has been
425 financially supported by the Project of Strategic Interest NextData PNR 2011–2013 (www.nextdataproject.it),
426 ERC Consolidator Grant (Project ID: 68323) “TIMED” Testing the role of

427 Mediterranean thermohaline circulation as a sensor of transient climate events and shaker of
428 North Atlantic Circulation", and MISTRALS/ PaleoMex program led by INSU/CNRS.

429

430 **References**

431 Andruleit H, Rogalla U and Stäger S (2005) Living coccolithophores recorded during the
432 onset of upwelling conditions off Oman in the western Arabian Sea. *J. Nannoplankton Res.* 2
433 27(1): 1–14.

434 Artegiani A, Paschini E, Russo A, Bregant D, Raicich F and Pinardi N (1997) The Adriatic
435 Sea General Circulation. Part II: Baroclinic Circulation Structure. *Journal of Physical*
436 *Oceanography* 27(8): 1515–1532: doi:10.1175/1520-
437 0485(1997)027<1515:TASGCP>2.0.CO;2.

438 Ausín B, Flores J-A, Sierro F-J, Bárcena M-A, Hernández-Almeida I, Francés G, et al. (2015)
439 Coccolithophore productivity and surface water dynamics in the Alboran Sea during the last
440 25kyr. *Palaeogeography, Palaeoclimatology, Palaeoecology* 418: 126–140:
441 doi:10.1016/j.palaeo.2014.11.011.

442 Balestra B, Marino M, Monechi S, Marano C and Locaiono F (2008) Coccolithophore
443 communities in the Gulf of Manfredonia (Southern Adriatic Sea): Data from water and
444 surface sediments. *Micropaleontology* 54(5): 377–396.

445 Barrera-Escoda A and Llasat MC (2015) Evolving flood patterns in a Mediterranean region
446 (1301/2012) and climatic factors; the case of Catalonia. *Hydrology and Earth System Sciences*
447 19(1): 465–483: doi:10.5194/hess-19-465-2015.

448 Baumann K-H, Andruleit H, Böckel B, Geisen M and Kinkel H (2005) The significance of
449 extant coccolithophores as indicators of ocean water masses, surface water temperature, and
450 paleoproductivity: a review. *Paläontologische Zeitschrift* 79(1): 93–112:
451 doi:10.1007/bf03021756.

452 Beaufort L (1997) Insolation Cycles as a Major Control of Equatorial Indian Ocean Primary

453 Production. *Science* 278(5342): 1451–1454: doi:10.1126/science.278.5342.1451.

454 Benito G, Macklin MG, Zielhofer C, Jones AF and Machado MJ (2015) Holocene flooding
455 and climate change in the Mediterranean. *CATENA* 130: 13–33:
456 doi:10.1016/j.catena.2014.11.014.

457 Bini M, Zanchetta G, Per oiu A, Cartier R, Català A, Cacho I, et al. (2019) The 4.2 ka BP
458 Event in the Mediterranean region: an overview. *Climate of the Past* 15(2): 555–577:
459 doi:10.5194/cp-15-555-2019.

460 Bonomo S, Cascella A, Alberico I, Ferraro L, Giordano L, Lirer F, et al. (2014)
461 Coccolithophores from near the Volturno estuary (central Tyrrhenian Sea). *Marine*
462 *Micropaleontology* 111: 26–37: doi:10.1016/j.marmicro.2014.06.001.

463 Bonomo S, Cascella A, Alberico I, Sorgato S, Pelosi N, Ferraro L, et al. (2016a) Reworked
464 Coccoliths as runoff proxy for the last 400years: The case of Gaeta Gulf (central Tyrrhenian
465 Sea, Central Italy). *Palaeogeography, Palaeoclimatology, Palaeoecology*. Elsevier B.V. 459:
466 15–28: doi:10.1016/j.palaeo.2016.06.037.

467 Bonomo S, Cascella A, Alberico I, Sorgato S, Pelosi N, Ferraro L, et al. (2016b) Reworked
468 Coccoliths as runoff proxy for the last 400 years: The case of Gaeta Gulf (central Tyrrhenian
469 Sea, Central Italy). *Palaeogeography, Palaeoclimatology, Palaeoecology* 459: 15–28:
470 doi:10.1016/j.palaeo.2016.06.037.

471 Bown P (1998) *Calcareous Nannofossil Biostratigraphy*. London: Kluwer Academic.

472 Bown PR, Dunkley Jones T, Young JR and Randell R (2009) A palaeogene record of extant
473 lower photic zone calcareous nannoplankton. *Palaeontology*: doi:10.1111/j.1475-
474 4983.2009.00853.x.

475 Broerse ATC, Ziveri P, van Hinte JE and Honjo S (2000) Coccolithophore export production,
476 species composition, and coccolith-CaCO₃ fluxes in the NE Atlantic. *Deep Sea Research*
477 *Part II: Topical Studies in Oceanography* 47(9–11): 1877–1905: doi:10.1016/S0967-
478 0645(00)00010-2.

479 Cacho I, Grimalt JO, Pelejero C, Canals M, Sierro FJ, Flores JA, et al. (1999) Dansgaard-
480 Oeschger and Heinrich event imprints in Alboran Sea paleotemperatures. *Paleoceanography*
481 14(6): 698–705: doi:10.1029/1999PA900044.

482 Cacho I, Grimalt JO, Sierro FJ, Shackleton N and Canals M (2000) Evidence for enhanced
483 Mediterranean thermohaline circulation during rapid climatic coolings. *Earth and Planetary*
484 *Science Letters* 183(3–4): 417–429: doi:10.1016/S0012-821X(00)00296-X.

485 Camuffo D and Enzi S (1996) The analysis of two bi-millennial series: Tiber and Po river
486 floods. *Climatic Variations and Forcing Mechanisms of the Last 2000 Years*. Berlin,
487 Heidelberg: Springer Berlin Heidelberg, 433–450: doi:10.1007/978-3-642-61113-1_20.

488 Caroli I and Caldara M (2007) Vegetation history of Lago Battaglia (eastern Gargano coast,
489 Apulia, Italy) during the middle-late Holocene. *Vegetation History and Archaeobotany* 16(4):
490 317–327: doi:10.1007/s00334-006-0045-y.

491 Cerino F, Malinverno E, Fornasaro D, Kralj M and Cabrini M (2017) Coccolithophore
492 diversity and dynamics at a coastal site in the Gulf of Trieste (northern Adriatic Sea).
493 *Estuarine, Coastal and Shelf Science*. Elsevier Ltd: doi:10.1016/j.ecss.2017.07.013.

494 Cisneros M, Cacho I, Frigola J, Canals M, Masqué P, Martrat B, et al. (2016) Sea surface
495 temperature variability in the central-western Mediterranean Sea during the last 2700 years: A
496 multi-proxy and multi-record approach. *Climate of the Past* 12(4): 849–869: doi:10.5194/cp-
497 12-849-2016.

498 Civitarese G, Gai M, Lipizer M and Eusebi Borzelli GL (2010) On the impact of the
499 Bimodal Oscillating System (BiOS) on the biogeochemistry and biology of the Adriatic and
500 Ionian Seas (Eastern Mediterranean). *Biogeosciences* 7(12): 3987–3997: doi:10.5194/bg-7-
501 3987-2010.

502 Civitarese G, Gai M, Vetrano A, Boldrin A, Bregant D, Rabitti S, et al. (1998)
503 Biogeochemical fluxes through the Strait of Otranto (Eastern Mediterranean). *Continental*
504 *Shelf Research*: doi:10.1016/S0278-4343(98)00016-8.

505 Combourieu-Nebout N, Peyron O, Bout-Roumazeilles V, Goring S, Dormoy I, Joannin S, et
506 al. (2013) Holocene vegetation and climate changes in the central Mediterranean inferred
507 from a high-resolution marine pollen record (Adriatic Sea). *Climate of the Past*:
508 doi:10.5194/cp-9-2023-2013.

509 Di Bella L, Frezza V, Bergamin L, Carboni MG, Falese F, Martorelli E, et al. (2014)
510 Foraminiferal record and high-resolution seismic stratigraphy of the Late Holocene
511 succession of the submerged Ombrone River delta (Northern Tyrrhenian Sea, Italy).
512 *Quaternary International* 328–329(1): 287–300: doi:10.1016/j.quaint.2013.09.043.

513 Di Rita F and Magri D (2009) Holocene drought, deforestation and evergreen vegetation
514 development in the central Mediterranean: A 5500 year record from Lago Alimini Piccolo,
515 Apulia, southeast Italy. *Holocene*: doi:10.1177/0959683608100574.

516 Dimiza MD, Triantaphyllou M V., Malinverno E, Psarra S, Karatsolis B-T, Mara P, et al.
517 (2015) The composition and distribution of living coccolithophores in the Aegean Sea (NE
518 Mediterranean). *Micropaleontology*.

519 Dimiza MD, Triantaphyllou MV V. and Dermitzakis MD (2008) Vertical distribution and
520 ecology of living coccolithophores in the marine ecosystems of Andros Island (Middle
521 Aegean Sea) during late summer 2001. *Hellenic Journal of Geosciences* 43: 1–7.

522 Faganeli J, Ga i M, Malej A and Smodlaka N (1989) Pelagic organic matter in the Adriatic
523 Sea in relation to winter hydrographic conditions. *Journal of Plankton Research*:
524 doi:10.1093/plankt/11.6.1129.

525 Ferreira J and Cachão M (2005) Calcareous nannoplankton from the Guadiana estuary and
526 Algarve continental shelf (southern Portugal). *Thalassas* 21(1): 35–44.

527 Ferreira J, Cachão M and González R (2008) Reworked calcareous nannofossils as ocean
528 dynamic tracers: The Guadiana shelf case study (SW Iberia). *Estuarine, Coastal and Shelf*
529 *Science* 79(1): 59–70: doi:10.1016/j.ecss.2008.03.012.

530 Flores JA, Gersonde RR, Sierro FJ and Niebler HS (2000) Southern ocean pleistocene

531 calcareous nannofossil events: Calibration with isotope and geomagnetic stratigraphies.
532 *Marine Micropaleontology* 40(4): 377–402: doi:10.1016/S0377-8398(00)00047-5.

533 Fonda Umani S (1996) Pelagic production and biomass in the Adriatic Sea. *Scientia Marina*.
534 Frigola J, Moreno a., Cacho I, Canals M, Sierro FJ, Flores J a., et al. (2007) Holocene climate
535 variability in the western Mediterranean region from a deepwater sediment record.
536 *Paleoceanography* 22(2): 1–16: doi:10.1029/2006PA001307.

537 Ga i M, Civitarese G, Kova evi V, Ursella L, Bensi M, Menna M, et al. (2014) Extreme
538 winter 2012 in the adriatic: An example of climatic effect on the biOS rhythm. *Ocean*
539 *Science*: doi:10.5194/os-10-513-2014.

540 Ga i M, Civitarese G, Miserocchi S, Cardin V, Crise A and Mauri E (2002) The open-ocean
541 convection in the Southern Adriatic: A controlling mechanism of the spring phytoplankton
542 bloom. *Continental Shelf Research*: doi:10.1016/S0278-4343(02)00050-X.

543 Gacic M, Eusebi Borzelli GL, Civitarese G, Cardin V and Yari S (2010) Can internal
544 processes sustain reversals of the ocean upper circulation? The Ionian Sea example.
545 *Geophysical Research Letters* 37(9): 1–5: doi:10.1029/2010GL043216.

546 Ga i M, Marullo S, Santoleri R and Bergamasco A (1997) Analysis of the seasonal and
547 interannual variability of the sea surface temperature field in the Adriatic Sea from AVHRR
548 data (1984-1992). *Journal of Geophysical Research: Oceans*. John Wiley & Sons, Ltd
549 102(C10): 22937–22946: doi:10.1029/97JC01720.

550 Giunta S, Negri a., Morigi C, Capotondi L, Combourieu-Nebout N, Emeis KC, et al. (2003)
551 Coccolithophorid ecostratigraphy and multi-proxy paleoceanographic reconstruction in the
552 Southern Adriatic Sea during the last deglacial time (Core AD91-17). *Palaeogeography,*
553 *Palaeoclimatology, Palaeoecology* 190: 39–59: doi:10.1016/S0031-0182(02)00598-9.

554 Godrijan J, Young JR, Mari Pfannkuchen D, Precali R and Pfannkuchen M (2018) Coastal
555 zones as important habitats of coccolithophores: A study of species diversity, succession, and
556 life-cycle phases. *Limnology and Oceanography*: doi:10.1002/lno.10801.

557 Gogou A, Triantaphyllou M, Xoplaki E, Izdebski A, Parinos C, Dimiza M, et al. (2016)
558 Climate variability and socio-environmental changes in the northern Aegean (NE
559 Mediterranean) during the last 1500 years. *Quaternary Science Reviews* 136: 209–228:
560 doi:10.1016/j.quascirev.2016.01.009.

561 Goudeau MLS, Reichert GJ, Wit JC, de Nooijer LJ, Grauel AL, Bernasconi SM, et al. (2015)
562 Seasonality variations in the Central Mediterranean during climate change events in the Late
563 Holocene. *Palaeogeography, Palaeoclimatology, Palaeoecology* 418: 304–318:
564 doi:10.1016/j.palaeo.2014.11.004.

565 Grauel AL and Bernasconi SM (2010) Core-top calibration of $\delta^{18}O$ and $\delta^{13}C$ of *G. ruber*
566 (white) and *U. mediterranea* along the southern Adriatic coast of Italy. *Marine*
567 *Micropaleontology*: doi:10.1016/j.marmicro.2010.09.003.

568 Grauel AL, Goudeau MLS, de Lange GJ and Bernasconi SM (2013) Climate of the past 2500
569 years in the Gulf of Taranto, central Mediterranean Sea: A high-resolution climate
570 reconstruction based on $\delta^{18}O$ and $\delta^{13}C$ of *Globigerinoides ruber* (white). *The Holocene* 23(10):
571 1440–1446: doi:10.1177/0959683613493937.

572 Guerreiro C, Oliveira A, de Stigter H, Cachão M, Sá C, Borges C, et al. (2013) Late winter
573 coccolithophore bloom off central Portugal in response to river discharge and upwelling.
574 *Continental Shelf Research* 59: 65–83: doi:10.1016/j.csr.2013.04.016.

575 Hagino K, Okada H and Matsuoka H (2000) Spatial dynamics of coccolithophore
576 assemblages in the Equatorial Western-Central Pacific Ocean. *Marine Micropaleontology*:
577 doi:10.1016/S0377-8398(00)00014-1.

578 Haidar AT and Thierstein HR (2001) Coccolithophore dynamics off Bermuda (N. Atlantic).
579 *Deep-Sea Research Part II: Topical Studies in Oceanography* 48(8–9): 1925–1956:
580 doi:10.1016/S0967-0645(00)00169-7.

581 Honjo S and Okada H (1974) Community structure of coccolithophores in the photic layer of
582 the mid-Pacific. *Micropaleontology* 20(2): 209–230.

583 Hurrell JW (1995) Decadal Trends in the North Atlantic Oscillation: Regional Temperatures
584 and Precipitation. *Science* 269(5224): 676–679: doi:10.1126/science.269.5224.676.

585 Ilijani N, Miko S, Petrincec B and Frani Z (2014) Metal deposition in deep sediments from
586 the Central and South Adriatic Sea. *Geologia Croatica*: doi:10.4154/gc.2014.14.

587 Incarbona A, Bonomo S, Di Stefano E, Zgozi S, Essarbout N, Talha M, et al. (2008)
588 Calcareous nannofossil surface sediment assemblages from the Sicily Channel (central
589 Mediterranean Sea): Palaeoceanographic implications. *Marine Micropaleontology* 67(3–4):
590 297–309: doi:10.1016/j.marmicro.2008.03.001.

591 Incarbona A, Martrat B, Mortyn PG, Sprovieri M, Ziveri P, Gogou A, et al. (2016)
592 Mediterranean circulation perturbations over the last five centuries: Relevance to past Eastern
593 Mediterranean Transient-type events. *Scientific Reports* 6(1): 29623: doi:10.1038/srep29623.

594 Incarbona A, Ziveri P, Di Stefano E, Lirer F, Mortyn G, Patti B, et al. (2010) Calcareous
595 nannofossil assemblages from the Central Mediterranean Sea over the last four centuries: the
596 impact of the little ice age. *Climate of the Past Discussions* 6(3): 817–866: doi:10.5194/cpd-
597 6-817-2010.

598 Jalali B, Sicre M-A, Bassetti M-A and Kallel N (2016) Holocene climate variability in the
599 North-Western Mediterranean Sea (Gulf of Lions). *Climate of the Past* 12(1): 91–101:
600 doi:10.5194/cp-12-91-2016.

601 Jalali B, Sicre M-A, Klein V, Schmidt S, Maselli V, Lirer F, et al. (2018) Deltaic and Coastal
602 Sediments as Recorders of Mediterranean Regional Climate and Human Impact Over the Past
603 Three Millennia. *Paleoceanography and Paleoclimatology*. John Wiley & Sons, Ltd 33(6):
604 579–593: doi:10.1029/2017PA003298.

605 Kaplan JO, Krumhardt KM and Zimmermann N (2009) The prehistoric and preindustrial
606 deforestation of Europe. *Quaternary Science Reviews*: doi:10.1016/j.quascirev.2009.09.028.

607 Kouli K, Gogou A, Bouloubassi I, Triantaphyllou MV, Ioakim C, Katsouras G, et al. (2012)
608 Late postglacial paleoenvironmental change in the northeastern Mediterranean region:

609 Combined palynological and molecular biomarker evidence. *Quaternary International* 261:
610 118–127: doi:10.1016/j.quaint.2011.10.036.

611 Leider A, Hinrichs KU, Mollenhauer G and Versteegh GJM (2010) Core-top calibration of
612 the lipid-based U37K and TEX86 temperature proxies on the southern Italian shelf (SW
613 Adriatic Sea, Gulf of Taranto). *Earth and Planetary Science Letters*:
614 doi:10.1016/j.epsl.2010.09.042.

615 Lirer F, Sprovieri M, Ferraro L, Vallefucoco M, Capotondi L, Cascella A, et al. (2013)
616 Integrated stratigraphy for the Late Quaternary in the eastern Tyrrhenian Sea. *Quaternary
617 International* 292: 71–85: doi:10.1016/j.quaint.2012.08.2055.

618 Lirer F, Sprovieri M, Vallefucoco M, Ferraro L, Pelosi N, Giordano L, et al. (2014) Planktonic
619 foraminifera as bio-indicators for monitoring the climatic changes that have occurred over the
620 past 2000 years in the southeastern Tyrrhenian Sea. *Integrative Zoology* 9(4): 542–554:
621 doi:10.1111/1749-4877.12083.

622 Ljubimir S, Jasprica N, Ali M, Hrustić E, Dupić I, Radić I, Čar A, et al. (2017) Interannual
623 (2009–2013) variability of winter-spring phytoplankton in the open South Adriatic Sea:
624 Effects of deep convection and lateral advection. *Continental Shelf Research* 143: 311–321:
625 doi:10.1016/j.csr.2017.05.007.

626 López-Moreno JJ, Vicente-Serrano SM, Morán-Tejeda E, Lorenzo-Lacruz J, Kenawy A and
627 Beniston M (2011a) Effects of the North Atlantic Oscillation (NAO) on combined
628 temperature and precipitation winter modes in the Mediterranean mountains: Observed
629 relationships and projections for the 21st century. *Global and Planetary Change*:
630 doi:10.1016/j.gloplacha.2011.03.003.

631 López-Moreno JJ, Vicente-Serrano SM, Moran-Tejeda E, Zabalza J, Lorenzo-Lacruz J and
632 García-Ruiz JM (2011b) Impact of climate evolution and land use changes on water yield in
633 the Ebro basin. *Hydrology and Earth System Sciences* 15(1): 311–322: doi:10.5194/hess-15-
634 311-2011.

635 Lowe JJ, Blockley S, Trincardi F, Asioli A, Cattaneo A, Matthews IP, et al. (2007) Age
636 modelling of late Quaternary marine sequences in the Adriatic: Towards improved precision
637 and accuracy using volcanic event stratigraphy. *Continental Shelf Research* 27(3–4): 560–
638 582: doi:10.1016/j.csr.2005.12.017.

639 Malinverno E, Triantaphyllou M V., Stavrakakis S, Ziveri P and Lykousis V (2009) Seasonal
640 and spatial variability of coccolithophore export production at the South-Western margin of
641 Crete (Eastern Mediterranean). *Marine Micropaleontology*. Elsevier B.V. 71(3–4): 131–147:
642 doi:10.1016/j.marmicro.2009.02.002.

643 Malinverno E, Ziveri P and Corselli C (2003) Coccolithophorid distribution in the Ionian Sea
644 and its relationship to eastern Mediterranean circulation during late fall to early winter 1997.
645 *Journal of Geophysical Research* 108(C9): 2156–2202: doi:10.1029/2002JC001346.

646 Manca BB, Kovaevi V, Gai M and Viezzoli D (2002) Dense water formation in the Southern
647 Adriatic Sea and spreading into the Ionian Sea in the period 1997-1999. *Journal of Marine*
648 *Systems*: doi:10.1016/S0924-7963(02)00056-8.

649 Marchini G, Zanchetta G, Santacroce R, Vigliotti L, Capotondi L and Sulpizio R (2014)
650 Tephrostratigraphy of Marine Core AD91-17 (Adriatic Sea) Revised. *Alpine and*
651 *Mediterranean Quaternary*.

652 Margaritelli G, Cisneros M, Cacho I, Capotondi L, Vallefucoco M, Rettori R, et al. (2018)
653 Climatic variability over the last 3000 years in the central - western Mediterranean Sea
654 (Menorca Basin) detected by planktonic foraminifera and stable isotope records. *Global and*
655 *Planetary Change* 169: 179–187: doi:10.1016/j.gloplacha.2018.07.012.

656 Margaritelli G, Vallefucoco M, Di Rita F, Bellucci L, Insinga DD, Petrosino P, et al. (2016)
657 Climate events from a shallow water marine record of the Central Tyrrhenian during the last
658 four millennia. *Global and Planetary Change* 141: doi:10.1016/j.gloplacha.2016.04.007.

659 Martrat B, Grimalt JO, Lopez-Martinez C, Cacho I, Sierro FJ, Flores JA, et al. (2004) Abrupt
660 temperature changes in the Western Mediterranean over the past 250,000 years. *Science (New*

661 York, N.Y.) 306(5702): 1762–1765: doi:10.1126/science.1101706.

662 Matthews IP, Trincardi F, Lowe JJ, Bourne AJ, MacLeod A, Abbott PM, et al. (2015)

663 Developing a robust tephrochronological framework for Late Quaternary marine records in

664 the Southern Adriatic Sea: New data from core station SA03-11. *Quaternary Science*

665 *Reviews*: doi:10.1016/j.quascirev.2014.10.009.

666 Moreno A, Pérez A, Frigola J, Nieto-Moreno V, Rodrigo-Gámiz M, Martrat B, et al. (2012)

667 The Medieval Climate Anomaly in the Iberian Peninsula reconstructed from marine and lake

668 records. *Quaternary Science Reviews*: doi:10.1016/j.quascirev.2012.04.007.

669 Narciso Á, Flores J-A, Cachão M, Piva A, Asioli A, Andersen N, et al. (2012) Late Glacial–

670 Holocene transition in the southern Adriatic Sea: Coccolithophore and Foraminiferal

671 evidence. *Micropaleontology* 58(6): 523–538: doi:10.2307/24413309.

672 Oldfield F, Asioli A, Accorsi CA, Mercuri AM, Juggins S, Langone L, et al. (2003) A high

673 resolution late Holocene palaeo environmental record from the central Adriatic Sea.

674 *Quaternary Science Reviews* 22(2–4): 319–342: doi:10.1016/S0277-3791(02)00088-4.

675 Pérez-Folgado M, Sierro FJ, Flores J a., Grimalt JO and Zahn R (2004) Paleoclimatic

676 variations in foraminifer assemblages from the Alboran Sea (Western Mediterranean) during

677 the last 150 ka in ODP Site 977. *Marine Geology* 212(1–4): 113–131:

678 doi:10.1016/j.margeo.2004.08.002.

679 Pinardi N, Zavatarelli M, Adani M, Coppini G, Fratianni C, Oddo P, et al. (2015)

680 Mediterranean Sea large-scale low-frequency ocean variability and water mass formation

681 rates from 1987 to 2007: A retrospective analysis. *Progress in Oceanography* 132: 318–332:

682 doi:10.1016/j.pocean.2013.11.003.

683 Piva A, Asioli a., Trincardi F, Schneider RR and Vigliotti L (2008) Late-Holocene climate

684 variability in the Adriatic Sea (Central Mediterranean). *The Holocene* 18(1): 153–167:

685 doi:10.1177/0959683607085606.

686 Reale M, Crise A, Farneti R and Mosetti R (2016) A process study of the Adriatic-Ionian

687 System baroclinic dynamics. *Journal of Geophysical Research: Oceans*:
688 doi:10.1002/2016JC011763.

689 Rodrigo-Gámiz M, Martínez-Ruiz F, Jiménez-Espejo FJ, Gallego-Torres D, Nieto-Moreno V,
690 Romero O, et al. (2011) Impact of climate variability in the western Mediterranean during the
691 last 20,000 years: Oceanic and atmospheric responses. *Quaternary Science Reviews*. Elsevier
692 Ltd 30(15–16): 2018–2034: doi:10.1016/j.quascirev.2011.05.011.

693 Rohling E, Mayewski P, Abu-Zied R, Casford J and Hayes A (2002) Holocene atmosphere-
694 ocean interactions: Records from Greenland and the Aegean sea. *Climate Dynamics* 18(7):
695 587–594: doi:10.1007/s00382-001-0194-8.

696 Rohling EJ, Marino G and Grant KM (2015) Mediterranean climate and oceanography, and
697 the periodic development of anoxic events (sapropels). *Earth-Science Reviews* 143:
698 doi:10.1016/j.earscirev.2015.01.008.

699 Sangiorgi F, Capotondi L, Combourieu Nebout N, Vigliotti L, Brinkhuis H, Giunta S, et al.
700 (2003) Holocene seasonal sea-surface temperature variations in the southern Adriatic Sea
701 inferred from a multiproxy approach. *Journal of Quaternary Science*: doi:10.1002/jqs.782.

702 Sbaffi L, Wezel FC, Kallel N, Paterne M, Cacho I, Ziveri P, et al. (2001) Response of the
703 pelagic environment to palaeoclimatic changes in the central Mediterranean Sea during the
704 Late Quaternary. *Marine Geology* 178(1–4): 39–62: doi:10.1016/S0025-3227(01)00185-2.

705 Schwab C, Kinkel H, Weinelt M and Repschlger J (2012) Coccolithophore paleoproductivity
706 and ecology response to deglacial and Holocene changes in the Azores Current System.
707 *Paleoceanography*: doi:10.1029/2012PA002281.

708 Sellschopp J and Álvarez A (2003) Dense low-salinity outflow from the Adriatic Sea under
709 mild (2001) and strong (1999) winter conditions. *Journal of Geophysical Research*. John
710 Wiley & Sons, Ltd 108(C9): 8104: doi:10.1029/2002JC001562.

711 Shabrang L, Menna M, Pizzi C, Lavigne H, Civitarese G and Ga i M (2016) Long-term
712 variability of the southern Adriatic circulation in relation to North Atlantic Oscillation. *Ocean*

713 *Science* 12(1): 233–241: doi:10.5194/os-12-233-2016.

714 Siani G, Magny M, Paterne M, Debret M and Fontugne M (2013) Paleohydrology
715 reconstruction and Holocene climate variability in the South Adriatic Sea. *Climate of the Past*
716 9(1): 499–515: doi:10.5194/cp-9-499-2013.

717 Sicre M-A, Bard E, Ezat U and Rostek F (2002) Alkenone distributions in the North Atlantic
718 and Nordic sea surface waters. *Geochemistry, Geophysics, Geosystems* 3(2): 1 of 13–13 13:
719 doi:10.1029/2001GC000159.

720 Sicre M-A, Jalali B, Martrat B, Schmidt S, Bassetti M-A and Kallel N (2016) Sea surface
721 temperature variability in the North Western Mediterranean Sea (Gulf of Lion) during the
722 Common Era. *Earth and Planetary Science Letters*. Elsevier 456: 124–133:
723 doi:10.1016/J.EPSL.2016.09.032.

724 Sierro FJ, Hodell D a., Curtis JH, Flores J a., Reguera I, Colmenero-Hidalgo E, et al. (2005)
725 Impact of iceberg melting on Mediterranean thermohaline circulation during Heinrich events.
726 *Paleoceanography* 20(2): 1–13: doi:10.1029/2004PA001051.

727 Simoncelli S, Masina S, Axell L, Liu Y, Salon S, Cossarini G, et al. (2016) MyOcean regional
728 reanalyses: overview of reanalyses systems and main results. *Mercator Ocean Journal* 43.

729 Skampa E, Triantaphyllou M V., Dimiza MD, Gogou A, Malinverno E, Stavrakakis S, et al.
730 (2019) Coupling plankton - sediment trap - surface sediment coccolithophore regime in the
731 North Aegean Sea (NE Mediterranean). *Marine Micropaleontology*:
732 doi:10.1016/j.marmicro.2019.03.001.

733 Skeji S, Arapov J, Kova evi V, Bužan i M, Bensi M, Giani M, et al. (2018)
734 Coccolithophore diversity in open waters of the middle Adriatic Sea in pre- and post-winter
735 periods. *Marine Micropaleontology*: doi:10.1016/j.marmicro.2018.07.006.

736 Sprovieri R, Di Stefano E, Incarbona A and Gargano ME (2003) A high-resolution record of
737 the last deglaciation in the Sicily Channel based on foraminifera and calcareous nannofossil
738 quantitative distribution. *Palaeogeography, Palaeoclimatology, Palaeoecology* 202(1–2):

739 119–142: doi:10.1016/S0031-0182(03)00632-1.

740 Sprovieri R, Di Stefano E, Incarbona A and Oppo DW (2006) Suborbital climate variability
741 during Marine Isotopic Stage 5 in the central Mediterranean basin: evidence from calcareous
742 plankton record. *Quaternary Science Reviews* 25(17–18): 2332–2342:
743 doi:10.1016/j.quascirev.2006.01.035.

744 Theocharis A, Krokos G, Velaoras D and Korres G (2014) An Internal Mechanism Driving
745 the Alternation of the Eastern Mediterranean Dense/Deep Water Sources. American
746 Geophysical Union (AGU), 113–137: doi:10.1002/9781118847572.ch8.

747 Totti C, Civitarese G, Acri F, Barletta D, Candelari G, Paschini E, et al. (2000) Seasonal
748 variability of phytoplankton populations in the middle Adriatic sub-basin. *Journal of Plankton*
749 *Research*. Oxford University Press 22(9): 1735–1756: doi:10.1093/plankt/22.9.1735.

750 Triantaphyllou M V., Dimiza MD, Krasakopoulou E, Malinverno E, Lianou V and
751 Souvermezoglou E (2010) Seasonal variation in *Emiliana huxleyi* coccolith morphology and
752 calcification in the Aegean Sea (Eastern Mediterranean). *Geobios* 43(1): 99–110:
753 doi:10.1016/j.geobios.2009.09.002.

754 Triantaphyllou M V., Gogou A, Dimiza MD, Kostopoulou S, Parinos C, Roussakis G, et al.
755 (2016a) Holocene Climatic Optimum centennial-scale paleoceanography in the NE Aegean
756 (Mediterranean Sea). *Geo-Marine Letters* 36(1): 51–66: doi:10.1007/s00367-015-0426-2.

757 Triantaphyllou M V., Karatsolis B, Dimiza MD, Malinverno E, Cerino F, Psarra S, et al.
758 (2016b) Coccolithophore combination coccospheres from the NE Mediterranean Sea: new
759 evidence and taxonomic revisions. *Micropaleontology* 61(6): 457–472.

760 Triantaphyllou M V., Ziveri P, Gogou A, Marino G, Lykousis V, Bouloubassi I, et al. (2009)
761 Late Glacial-Holocene climate variability at the south-eastern margin of the Aegean Sea.
762 *Marine Geology* 266(1–4): 182–197: doi:10.1016/j.margeo.2009.08.005.

763 Trouet V, Esper J, Graham NE, Baker A, Scourse JD and Frank DC (2009) Persistent positive
764 North Atlantic oscillation mode dominated the Medieval Climate Anomaly. *Science (New*

765 York, N.Y.) 324(5923): 78–80: doi:10.1126/science.1166349.

766 Vallefuoco M, Lirer F, Ferraro L, Pelosi N, Capotondi L, Sprovieri M, et al. (2012) Climatic
767 variability and anthropogenic signatures in the Gulf of Salerno (southern-eastern Tyrrhenian
768 Sea) during the last half millennium. *Rendiconti Lincei* 23(1): 13–23: doi:10.1007/s12210-
769 011-0154-0.

770 Vilibi I, Matijevi S, Šepi J and Kušpili G (2012) Changes in the Adriatic oceanographic
771 properties induced by the Eastern Mediterranean Transient. *Biogeosciences*: doi:10.5194/bg-
772 9-2085-2012.

773 Wirth SB, Glur L, Gilli A and Anselmetti FS (2013) Holocene flood frequency across the
774 Central Alps – solar forcing and evidence for variations in North Atlantic atmospheric
775 circulation. *Quaternary Science Reviews* 80: 112–128: doi:10.1016/j.quascirev.2013.09.002.

776 Ziveri P, Baumann KH, Böckel B, Bollmann J and Young JR (2004) Biogeography of
777 selected Holocene coccoliths in the Atlantic Ocean. *Coccolithophores: from molecular*
778 *process to global impact*, 403–428: doi:10.1007/978-3-662-06278-4_15.

779

780